

## Chapter 3<sup>1</sup>

# Deep Space Station 12: Echo

The Echo site, at Goldstone, California, has been in operation since 1960 and is named for its initial operational support of Project Echo, an experiment that transmitted voice communications coast to coast by bouncing signals off the surface of a passive balloon-type satellite. The original 26-m antenna erected for the Echo experiment was moved in 1962 to the nearby Venus site.

The present Echo antenna, originally 26 m in diameter, was erected in late 1962 and was extended to 34 m in 1979. The antenna was patterned after radio-astronomy antennas then in use at the Carnegie Institution of Washington (D.C.) and the University of Michigan. The main features borrowed from the radio-astronomy antenna design are the mount and the celestial-coordinate pointing system. The axis of the polar, or hour-angle gear wheel, which moves the antenna east and west, is parallel to the polar axis of Earth and points precisely at Polaris, the North Star. The declination gear wheel, which moves the antenna north and south, is mounted on an axis that parallels Earth's equator. A spacecraft in deep space appears in the sky much like any celestial object, rising in the east and setting in the west, generally 7 to 14 hours later. The desirable feature of the polar-mount antenna is that (usually) once the declination angle has been set, only the hour-angle gear wheel is driven in order to track the spacecraft. The rate of movement, which counteracts Earth's rotation rate, is approximately 0.004 deg/s. Figure 3-1 is a photograph of the Echo antenna.

The Echo antenna stands approximately 35-m high and weighs approximately 270,000 kg. The operating speed ranges from 0.25 deg/s down to

---

<sup>1</sup>Based on "Evolution of the Deep Space Network 34-M Diameter Antennas," by William A. Imbriale, which appeared in *Proceedings of the IEEE Aerospace Conference*, Snowmass, Colorado, March 21–28, 1998. (© 1998 IEEE)



**Fig. 3-1. Photograph of the Echo antenna.**

0.001 deg/s. The antenna can be operated automatically or manually and has a pointing accuracy of 0.020 deg in winds up to 70 km/h.

As did the entire DSN, DSS-12 began operation at the 960-MHz L-band frequency chosen for the Pioneer 3 and 4 lunar missions. It was equipped with a 890–960-MHz linearly polarized feed horn and a 10-kW transmitter.

In mid-1962, Eberhardt Rechtin recommended the development of an S-band (2.110–2.120 GHz transmit and 2.29–2.30 GHz receive) configuration as a standard for the DSN [1]. S-band was chosen, both because of the availability of the spectrum and the frequency's application to future deep-space communications design. For example, galactic background noise was high at L-band. The higher S-band frequency decreases the noise while providing additional advantages by increasing the gain of spacecraft antennas. Therefore, the Echo site was converted to S-band in 1965.

An important requirement of the conversion was a closed-loop device for automatically pointing the antennas at a space probe. In order to track the space probe automatically, the antenna had to possess an electrical feed capable of using the space probe signal for driving the servo control system. An S-band Cassegrain monopulse (SCM) feed horn provides this capability.

### 3.1 The S-Band Cassegrain Monopulse Feed Horn

An SCM feed horn [2–4], developed for incorporation into the Cassegrain cone assembly, was designed and built to convert the 26-m Echo antenna to S-band. The feed horn contains both a sum channel for telemetry reception and a difference channel to provide error signals for antenna pointing. The multimode monopulse feed horn uses the basic (transverse electric)  $TE_{10}$  mode to provide a reference (sum) channel radiation. In addition, the  $TE_{12}$ , (transverse magnetic)  $TM_{12}$ , and  $TE_{30}$  modes are used for feed sidelobe suppression. The sum pattern gain enables a larger portion of the feed energy to reside in the main beam, thus minimizing the feed forward spillover losses. Monopulse capability is achieved in the same feed horn by combining the  $TE_{11}$  and  $TM_{11}$  modes to form the E-plane difference pattern, and the  $TE_{20}$  mode for the H-plane difference pattern.

To produce the desired patterns, the relative phase and amplitude of the modes must be generated and controlled by the monopulse circuitry. These modes must also be matched into the multimode feed horn. The monopulse bridge that feeds the common-aperture section is a standard four-guide monopulse circuit providing dual polarization. More details of the feed design and performance measurements are given in [2–4].

After development of the feed design, a contract was awarded to the Hughes Aircraft Company to fabricate the SCM cone assemblies for use on the 26-m antennas. The cone assembly consisted of the feed horn and monopulse circuitry, the S-band traveling-wave maser (TWM), and a diplexer to provide for the 10-kW transmitter input. Table 3-1 presents aperture efficiency and antenna gain data for four different antennas on three continents. The Pioneer antenna (DSS-11) was the oldest antenna in the DSN and had the poorest surface, and the Canberra (Australia) antenna (DSS-42) had the first precision surface to be used by the DSN. Thus, the apparent variation in aperture efficiency between antennas has some correlation with known antenna characteristics and does not necessarily reflect a difference in the four SCM cone assemblies involved.

**Table 3-1. Antenna aperture efficiency and gain at 2.295 GHz, SCM feed system.**

Parameter	Deep Space Station			
	11	41	42	51
Aperture efficiency (%)	51	55	58	52
Aperture efficiency (dB)	-2.92	-2.59	-2.37	-2.84
Antenna gain (dB)	53.0	53.3	53.5	53.0

The efficiencies and gains given in Table 3-1 were measured at the SCM sum channel selector switches, and with a small correction for the total losses between the feed horn and maser (estimated to be 0.18 dB), the actual antenna gain at the feed-horn output is about  $53.4 \pm 0.3$  dB, or an aperture efficiency of about  $57 \pm 4$  percent. The complete system temperature of the SCM cone assembly with the TWM has been determined to be  $42 \pm 3$  K with the antenna at zenith. The antenna temperature, measured at the SCM feed output, has been determined to be approximately 13 K.

### 3.2 The 26-Meter S-/X-Band Conversion Project

The addition of X-band receive (8.4–8.5 GHz) capability to the existing 26-m stations was in response to the support requirements for the outer planet missions. Due to the vastly increased distances from Earth, high frequencies must be employed by the spacecraft and the DSN to determine spacecraft trajectory and to achieve a greater data return. Also, several spacecraft require 64-m station support from the same area of the sky due to the combination of very long flight times and the relative position of the planets, which enables the use of intervening gravity-assist trajectories. The solution to alleviating the 64-m station overload was to increase the X-band capability of the DSN, either by adding stations or by converting existing S-band-only stations to S-/X-band capability. The latter, more economical, approach was selected [5].

The extension of the antenna diameter to 34 m provided a level of X-band performance sufficient to partially alleviate the 64-m subnet overload by (a) supporting S-/X-band navigation data acquisition out to the planet Saturn and (b) simultaneously providing a usable real-time video capability out to the planet Jupiter. This antenna diameter also proved to be the smallest diameter size suitable for arraying with the 64-m antenna.

The radio frequency (RF) modifications to the antenna system primarily included increasing the aperture diameter from 26 to 34 m and adding a simultaneous S-/X-band capability. The new redesign included a reflex-dichroic feed system similar to the one being used on the 64-m subnet [6]. In the 34-m case, a single new Cassegrain feed-horn housing, large enough to enclose both the S-band and X-band feed systems, was designed [7]. In order to minimize aperture blockage, the feed-horn focal point location was substantially moved toward the parabolic vertex and offset from the paraboloid axis. As a result, a new subreflector and quadripod were required.

Figure 3-2 details the S-/X-band feed geometry. Figure 3-3 shows a photo of the feed system. The original 26-m-diameter paraboloid focal length of 432 in. (10.97 m) is maintained and new outer panels according to the required contour are added. The initial 26-m system  $F/D$  ratio of 0.4235 is, therefore,

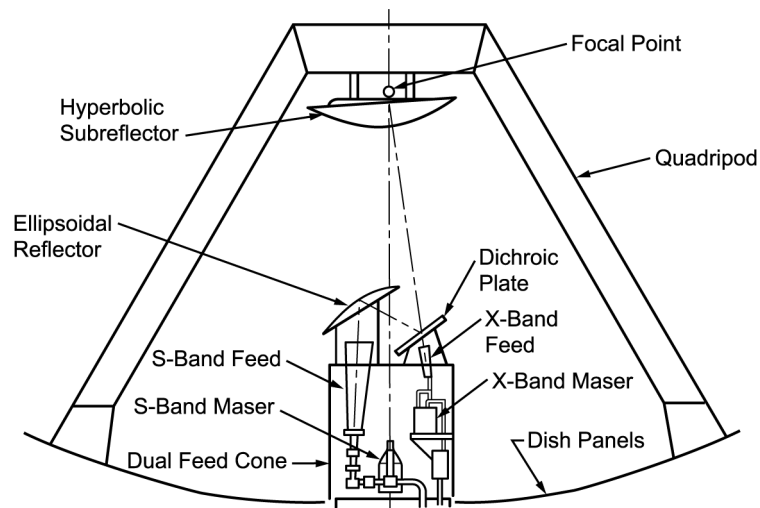
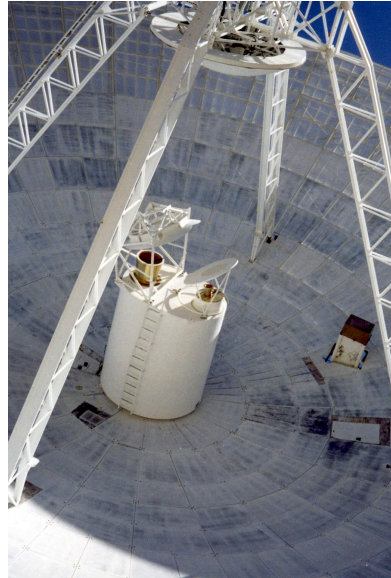


Fig. 3-2. The S-/X-band feed system.

substantially reduced to a new value of 0.3227, yielding a much deeper dish. In order to minimize central blockage caused by the substantial size of the single large feed cone and associated reflex-dichroic reflectors, the original design value for the separation of primary and secondary focal points of 228 in. (5.79 m) was increased to 276 in. (7.01 m). This results in a feed-horn position above the paraboloid vertex 48.0 in. (121.92 cm) lower than in the previous 26-m designs. In contrast to the 64-m system, where the subreflector is rotatable about the paraboloid axis (to obtain switching along the three separate feed horns used in that system), the 34-m design uses a fixed subreflector, permanently focused upon the X-band feed-horn focal point, located below the dichroic plate. Four of the elements—the S- and X-band feed horns, the ellipsoidal reflector, and the planar dichroic reflector—as well as the critical relative positions of the four elements, are borrowed directly from the previous 64-m designs [8,9].

With these critical positions held constant, the final optics design was determined by rotating the subassembly about the primary focal point at the radius value equal to 276 in. (7.01 m) until an approximately equal central blockage condition was achieved. This occurred with an offset angle of 7.6677 deg. This offset angle then determined the design of the subreflector.

The subreflector consists of three parts: the hyperboloidal surface contour, the nonoptic peripheral flange, and the nonoptic vertex plate. The peripheral flange was iteratively designed using computed scattered patterns, taking into account the decrease in power spilled past the rim of the paraboloid at both S- and X-bands. This is a key parameter in determining the noise performance



**Fig. 3-3. The feed system.**

of the finished design. The vertex plate was added to decrease RF illumination into the central zone, containing the feed horn and reflex reflectors.

### **3.2.1 Performance Predictions**

A detailed description of the methods used for analysis of the computed performance is given in [10] and will only be briefly summarized along with the presentation of the final results. The basic analysis technique uses the physical optics algorithm to determine the scattering from the reflecting surfaces. For S-band, starting with the E- and H-plane radiation patterns from a standard Jet Propulsion Laboratory (JPL) corrugated conical feed horn, the feed horn patterns are scattered off the ellipsoidal reflector and flat plate. The output is then scattered off the subreflector, which includes a vertex plate and flange. The final output is then used to evaluate the overall illumination efficiency of the main paraboloid. It should be noted that a complex set of antenna patterns is used throughout this process, with azimuthal modes of  $m = 0$ ,  $m = 1$ ,  $m = 2$ , and  $m = 3$  included. This preserves and sums the beam asymmetry accumulation as it develops from each surface.

The azimuthal analysis of feed radiation patterns is well documented in previous literature [10], showing that only  $m = 1$  components of the pattern contribute to antenna gain. Energy contained in the  $m \neq 1$  components represents a degradation of antenna gain, and in a receive mode, a possible source of system-noise-temperature degradation.

The X-band system evaluation is much simpler because no asymmetric ellipsoid is present; the asymmetric subreflector introduces the need for azimuthal modal decomposition analysis. Using the antenna patterns that were generated as described above, and at each stage preserving the azimuthal modes  $m = 0, 1, 2,$  and  $3,$  the various antenna efficiency components are computed, as shown in Table 3-2.

The predicted paraboloid and subreflector surface tolerance ranges from a low of 0.58 mm at reasonable elevation angles, with no wind or thermal, to a maximum of 1.0 mm at 60-deg elevation, with wind and thermal distortion included. This maximum gives a gain loss at X-band of 0.51 dB and at S-band of 0.04 dB. The higher root-mean-square (rms) of 1.0 mm was used for the antenna gain in Table 3-2.

**Table 3-2. The 34-m reflex feed-system-gain theoretical calculations for S- and X-bands.**

Efficiency Component	X-Band (8.415 GHz)		S-Band (2.295 GHz)	
	Ratio	dB	Ratio	dB
Forward spillover	0.96005	-0.1771	0.98231	-0.0775
Real spillover	0.99568	-0.0188	0.99637	-0.0158
Nonuniform phase illumination	0.84289	-0.7423	0.83582	-0.7789
Nonuniform phase illumination	0.91297	-0.3954	0.96398	-0.1593
Cross polarization	0.99942	-0.0025	0.99975	-0.0011
Mode conversion ( $m = 1$ )	0.99038	-0.0420	0.97503	-0.1098
Central blockage	0.97710	-0.1006	0.96510	-0.1543
Quadripod blockage (optical)	0.91700	-0.3760	0.91700	-0.3760
Paraboloid/subreflector surface tolerance loss (1.0-mm rms)	0.88209	-0.5448	0.99096	-0.0394
Ellipsoid reflector tolerance loss (0.51-mm rms)	N/A <sup>a</sup>	N/A	0.99759	-0.0105
Transmission loss through planar reflector	0.9950	-0.0218	N/A	N/A
Waveguide dissipative loss	0.97570	-0.1070	0.97720	-0.1000
Overall efficiency	0.55870	-2.5290	0.65720	-1.8230
Gain for 100% efficiency	N/A	69.537	N/A	58.252
Overall gain (dB)	N/A	67.01	N/A	56.43

<sup>a</sup>Not applicable.

The gain values are defined at the input to the maser preamplifiers. The S-band gain as indicated in Table 3-2 is for the S-band low-noise system. The expected gain for the S-band diplex mode is 0.09 dB less. The expected tolerance for X-band is +0.3 dB to -0.9 dB, and the S-band gain tolerance is  $\pm 0.6$  dB. These tolerances include the major error sources that will be incurred during field measurements using natural radio sources. As stated in the section on azimuthal mode analysis, beam squint at S-band, due to higher-order mode generation as a result of the asymmetric design, will degrade S-band gain by 0.34 dB below the peak value indicated in Table 3-2. Thus, the operational system, assuming X-band beam peak pointing, is predicted to operate with +67.0-dB X-band gain and +56.1-dB S-band gain (low-noise path) or +56.0-dB S-band gain (diplex path).

### 3.2.2 Performance Measurements

It should be noted that when DSS-12 was first completed, a series of star tracks was performed to measure the gain and system temperature, the result of which showed the maximum gain to be 65.7 dB, significantly below the predicted value. To explore the problem, a 34-m X-band gain study team was formed in 1980. The team discovered that the quality of the outer panels of the main reflector was significantly worse than was believed when the panels were first delivered. Removing 14 of the 96 new panels and retesting those removed showed rms values ranging from 1.02 mm to 2.54 mm, with a composite value of 1.4 mm. This could account for 0.75 dB of the loss, so new panels were procured, installed, and aligned. Also, it was discovered that there was an incorrect map of subreflector position as a function of elevation angles. Consequently, each antenna was calibrated to provide a permanent optimum subreflector position map. After the above-mentioned corrections, results shown in Table 3-3 were obtained, where S-band = 2.290–2.300 GHz and X-band = 8.400–8.450 GHz. S-band polarization is selectable right-hand circular polarization (RCP), left-hand circular polarization (LCP), and manually rotatable linear; and X-band polarization is selectable RCP and LCP.

## 3.3 The Goldstone–Apple Valley Radio Telescope

In 1994, the Echo antenna was decommissioned and converted into a radio telescope to be utilized as an educational resource for school children throughout the country. Technicians removed unneeded equipment from the antenna and installed new cables and a radio-astronomy receiving system. At the same time, engineers adapted the DSN's remote-control software for use on the radio telescope and developed training materials on how to operate it.

**Table 3-3. Measured performance of the 34-m S-/X-band system.**

Predicted Performance	Measured Performance		
	DSS-12	DSS-42	DSS-61
S-band:			
Gain (56.1 +0.6/-0.6 dB)	56.6 dB	56.6 dB	56.3 dB
Temperature (27.5 ± 2.5 K)	27.4 K	27.4 K	27.5 K
X-band:			
Gain (66.9 +0.3/-0.9 dB)	66.6 dB	66.6 dB	66.3 dB
Temperature (25 ± 2.0 K)	23.7 K	22.3 K	18.5 K

The Goldstone–Apple Valley Radio Telescope (GAVRT) program is a curriculum-driven educational program operated by a partnership between the Lewis Center for Educational Research (LCER), NASA, JPL, and the Apple Valley (California) Unified School District. The GAVRT program offers the unique opportunity for first through twelfth graders across America to take control of a dedicated 34-m radio telescope to pursue legitimate scientific inquiry. By connecting via the Internet to “mission control” at LCER in Apple Valley, students assume command of the massive instrument located at NASA’s deep space communications complex at Goldstone to observe the Sun, stars, and other astronomical objects.

Students conduct actual scientific observations in radio astronomy. The data is then compiled and made available by JPL to scientists, astronomers, teachers, and students around the world. For each student astronomer, personal discovery is likely, and scientific discovery is possible.

## References

- [1] N. Renzetti, *A History of the Deep Space Network*, JPL TR 32-1533, Jet Propulsion Laboratory, Pasadena, California, September 1971.
- [2] *S-Band Cassegrain Monopulse (SCM) Cone Assembly Final Report*, JPL 64-319 (internal document), Jet Propulsion Laboratory, Pasadena, California, July 10, 1964.
- [3] *S-Band Acquisition Antenna System Final Report*, Document FR-64-14-109, Hughes Aircraft Company, Fullerton, California, June 12, 1964.

- [4] “S-Band Cassegrain Monopulse Feed Development,” *Space Programs Summary 37-33, Vol. III*, Jet Propulsion Laboratory, Pasadena, California, pp. 43–48.
- [5] V. B. Lobb, “26-Meter S-X Conversion Project,” *The Deep Space Network Progress Report 42-39*, vol. March and April 1977, [http://tmo.jpl.nasa.gov/progress\\_report/issues.html](http://tmo.jpl.nasa.gov/progress_report/issues.html) Accessed February 2002.
- [6] R. W. Hartop, “Dual Frequency Feed System for 26-meter Antenna Conversion,” *Deep Space Network Progress Report 42-40*, vol. May and June 1977, [http://tmo.jpl.nasa.gov/progress\\_report/issues.html](http://tmo.jpl.nasa.gov/progress_report/issues.html) Accessed February 2002.
- [7] R. W. Hartop, “Dual Frequency Feed Cone Assemblies for 34-Meter Antennas,” *Deep Space Network Progress Report 42-47*, vol. July and August 1978, [http://tmo.jpl.nasa.gov/progress\\_report/issues.html](http://tmo.jpl.nasa.gov/progress_report/issues.html) Accessed February 2002.
- [8] D. L. Nixon and D. Bathker, “S/X-Band Microwave Optics Design and Analysis for DSN 34-Meter Diameter Antenna,” *Deep Space Network Progress Report 42-41*, [http://tmo.jpl.nasa.gov/progress\\_report/issues.html](http://tmo.jpl.nasa.gov/progress_report/issues.html) Accessed February 2002.
- [9] P. D. Potter, *S- and X-Band RF Feed System*, vol. VIII, JPL TR 32-1526, Jet Propulsion Laboratory, Pasadena, California, pp. 53–60, April 15, 1972.
- [10] A. C. Ludwig, *Calculation of Scattered Patterns From Asymmetrical Reflectors*, JPL TR 32-1430, Jet Propulsion Laboratory, Pasadena, California, February 15, 1970.